HANDLING ANALYSES OF A VEHICLE FITTED WITH A ROLL-RESISTANT HYDRAULICALLY INTERCONNECTED SUSPENSION

Nong Zhang, Lifu Wang, and William Hu

School of Electrical, Mechanical and Mechatronic Systems, Faculty of Engineering and Information Technology, University of Technology, Sydney, Australia

e-mail address of lead author: lifu.wang@student.uts.edu.au

Abstract

Transient handling analyses of a sport utility vehicle (SUV) fitted with a roll-resistant hydraulically interconnected suspension is presented in this paper. SUVs have a greater likelihood to rollover due to higher center of gravity, and hydraulically interconnected suspensions (HIS) have been proven as one practical means to effectively improve vehicle anti-roll ability. The modeling of a vehicle fitted with a HIS consists of a 9 degrees-of-freedom (DOF) full-car model and a 34 DOF HIS model, dynamically coupled together through boundary conditions. Steering angle taken from the tests is used as input to the simulations. In field tests, vehicles with different anti-roll systems are put under test by driving through a series of pylons at a constant speed. Acceleration, pressure and displacement transducers are used to measure and evaluate vehicles performance. From tests, HIS shows a superior performance over anti-roll bars in resisting vehicle rolls. The pressure response of the hydraulic suspension closely matches the simulation results, and discussions are provided afterwards.

1. INTRODUCTION

Rollover accidents of SUVs are dangerous and often result in loss of lives. Good suspensions can greatly reduce vehicular rollover propensity during extreme maneuvers. Completely passive interconnected suspensions are becoming increasingly popular for passenger vehicles, due to its low cost and high reliability. A passive interconnected suspension system is one in which the motion (displacement, velocity) at one wheel station can produce forces at other wheel stations, which is generally realized through either mechanical or fluidical means. From kinematics point of view, four wheel vehicle suspensions have four modes: bounce, roll, pitch, and warp [1-4]. The vertical ride generally requires a soft bounce mode, while stiff roll and pitch modes are beneficial for inhibiting vehicle attitude during steering, braking, and acceleration. It has also been well accepted that the suspension warp mode should be as soft as possible for road-holding performance. These four fundamental modes are strongly coupled and hard for a conventional passive suspension system to deal with. For example, the use of passive anti-roll bars increase the roll stiffness but at the same time yields a stiffer suspension warp mode, which is undesirable.

Interconnected suspensions in a full car level have the theoretically potential ability to uncouple these four modes [1; 4] , and have advantages in adjusting stiffness/damping in each of roll, bounce, pitching and articulation modes. Interconnected suspensions have been proposed since the1920s [5]and have achieved commercially success, but have not received equal attention in the research community. Very recently, attention has been put into interconnected suspensions. A survey of passive interconnected suspension has been done in [6]. In [7], a comprehensive survey on recent suspension development is presented with a focus on interconnected suspensions.

Let’s start with mechanically interconnected suspension. The passive mechanical interconnections among the suspension units in a full-vehicle model have been developed and investigated for many years [3]. The full-vehicle mechanically interconnected suspensions could decouple the different suspension modes, in order to provide a more favourable compromise between ride and handling requirements. Designs are complex and the weight is considerable. It is also difficult to be tuned to adapt various road and operating conditions.

Unlike mechanical interconnected suspensions that are heavy and difficult to offer additional damping, fluidic suspension systems can offer viable options in improving mode properties. The fluidical interconnection can be realized through hydraulic fluids, pneumatic fluids, or a combination of the two. The first and third types of media are most common in the literature, and they are called hydraulically interconnected suspensions (HIS) and hydro-pneumatic suspensions. Full-vehicle fluidically coupled suspension systems have been investigated on the topics of pneumatically interconnected suspensions [8], hydraulically interconnected suspensions, [6; 9-12], hydro-pneumatic suspensions [2; 13-16], and interconnection configuration [1; 17]. Variable fluidically interconnected suspensions are developed and employed in different application.

Cao etc. [2; 13; 14; 18] investigated the dynamics of interconnected hydro-pneumatic suspensions at a full car level, particularly heavy vehicle applications. The hydro-pneumatic suspension systems have been employed in heavy military vehicles for nearly half a century. The fluidic couplings are realised through hydro-pneumatic struts [16; 19], which have compact design and are claimed to have larger effective working area than normal hydraulic cylinders. The struts provide considerable flexibility for various interconnection configurations among the hydraulic and pneumatic chambers, either hydraulically or pneumatically [18]. A general framework for designing and tuning is included in [2; 13].

Hydraulically interconnected suspensions have achieved commercial success. One example is Kinetic H2 suspension; originally developed by Australian company Kinetic Pty Ltd. Kinetic H2 suspensions typically contain four double-acting hydraulic cylinders in addition to the original vehicle suspensions. The cylinders are mounted on the car body and the piston rods are fixed on the wheel assemblies. The chambers in the cylinders are interconnected by hydraulic circuits, arranged to counter vehicle roll motion. Each circuit comprises elements such as damper valves, hydraulic accumulators, pipelines, fittings and flexible hoses. Kinetic Dynamic Suspension System (KDSS) is a successful commercial application of this kind of technology, and different versions are available in many applications, e.g., Lexus GX 470 and 200 Series Toyota Land Cruiser. The performance is reported in [12; 20].

Zhang & Smith [6; 9-11] recently studied the dynamics of HIS systems at a focused level into multi-body vibration theory and interconnected fluid dynamics. A systematic approach are proposed for studying hydraulically interconnected suspensions in both time and frequency domain. The finite element modeling of nonlinear hydraulic system is seamlessly connected to a mass-spring vehicle model through hydraulic-mechanical coupling, and the theoretical analyses are validated by laboratory experiments[21]. However, transient analysis of a typical SUV fitted with a HIS based on experimental tests has not been carried out yet. This paper further extended this research into field test.

2. MODELING OF THE FULL CAR FITTED WITH A HIS

In an effort to retain simplicity, whilst still accounting for fluid interconnections between wheel stations, a lumped-mass 9 degrees-of-freedom (DOF) full-car model, as shown in Fig. 1, is used in this study[21].

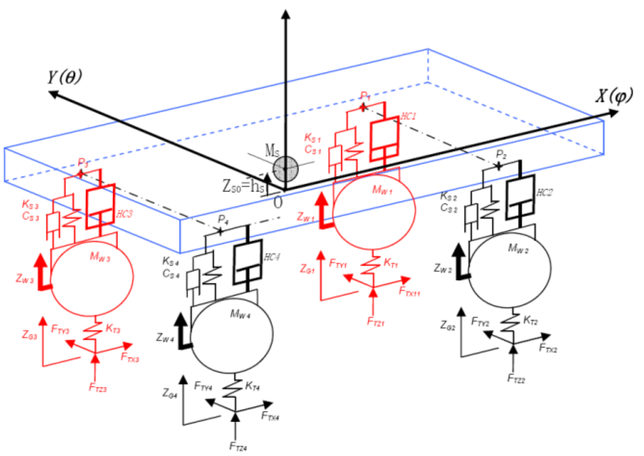

Figure 1 Schematic of a full-car with an HIS

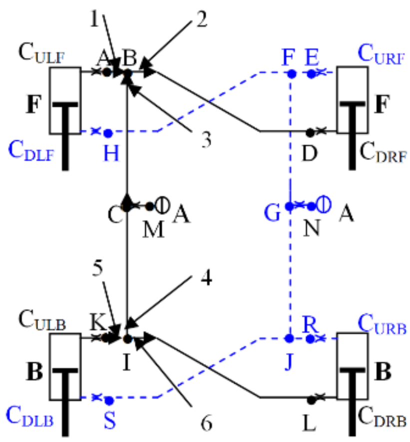

Figure 2 Schematic of a roll-resistant HIS

The vehicle system consists of linear tire damping and springing, linear conventional suspension springing, and a typical HIS system. The car body sprung mass is considered to have five DOF and each of the four wheel unsprung masses has only one DOF in vertical direction. From Figure 1, it can be seen that the shock absorbers of conventional independent suspensions between the sprung and unsprung masses are kept with the car. The added typical roll-resistant HIS arrangement for this application consists of two identical hydraulic circuits as shown in Figure 2. The two hydraulic circuits are coupled with each other kinetically via four identical double acting piston-cylinder actuators. Each of the hydraulic circuits comprises five damper valves, a nitrogen-filled diaphragm accumulator, and a hydraulic pipeline. The HIS circuits often include additional elements, such as hydraulic fittings and flexible hoses, but they fall beyond the consideration of this investigation. The FEM based numerical solution scheme is also briefly described.

Within the two hydraulic circuits, the cylinders are mounted on the car body and the piston rods are fixed on the wheel stations. The dynamic interaction between the hydraulic system and the sprung and unsprung masses can be described as such: relative velocities in the suspension struts cause fluid flows in both circuits and accompanying pressure changes in the cylinder chambers, which leads to new suspension strut forces being applied to the sprung and unsprung masses. As a result, vehicle body and wheel motions occur, which, in turn, affect the hydraulic system. This interaction will continue until the system reaches a new equilibrium. HIS systems can provide greater freedom to independently specify modal stiffness and damping characteristics. Ideally, HIS system function is characterized entirely by mode, though factors such as fluid compressibility and frequency-dependent hydraulic circuit impedance cause imperfect system function. The working mechanisms and features of the full-car HIS system can be found in [11].

3 STATE SPACE EQUATIONS

The details of derivation of the state space equations of the combined vehicle multi-body system and hydraulic circuits for transient analysis can be found in [11]. Here a brief description of the dynamic model, i.e., the state space representation of the integrated full-car system for the analysis of the transient responses caused by steering and road inputs is provided.

The state vector describing the motion of the sprung and unsprung lumped multi-body subsystem is defined as

$$X_M = [Z^T \ \dot{Z}^T]^T \tag{1}$$

where displacement vector is $Z = [\mathrm{Y_{V0}}\ \mathrm{Z_{V0}}\ \mathrm{Z_{W1}}\ \mathrm{Z_{W2}}\ \mathrm{Z_{W3}}\ \mathrm{Z_{W4}}\ \varphi_{\mathrm{XV}}\ \theta_{\mathrm{YV}}\ \psi_{\mathrm{ZV}}]^T$ (2)

and velocity vector is $\dot{Z} = [\dot{\mathrm{Y}}_{\mathrm{V0}}\ \dot{\mathrm{Z}}_{\mathrm{V0}}\ \dot{\mathrm{Z}}_{\mathrm{W1}}\ \dot{\mathrm{Z}}_{\mathrm{W2}}\ \dot{\mathrm{Z}}_{\mathrm{W3}}\ \dot{\mathrm{Z}}_{\mathrm{W4}}\ \dot{\varphi}_{\mathrm{XV}}\ \dot{\theta}_{\mathrm{YV}}\ \dot{\psi}_{\mathrm{ZV}}]^T$ (3)

The state vector describing the dynamic sates of the hydraulic subsystem is defined as

$$\begin{aligned} X_H = [&P_U^{C1}\ P_A^{AB}\ P_B^{AB}\ Q_B^{AB}\ P_M^{ABM}\ P_C^{BC}\ Q_C^{BC}\ Q_C^{CI}\ P_I^{CI}\ Q_I^{CI}\ Q_I^{IL}\ P_L^{IL}\ P_B^{C4}\ P_U^{C2}\ P_E^{EF}\ P_F^{EF}\ Q_F^{EF} \cdots \\ &P_N^{AFN} P_G^{FG}\ Q_G^{FG}\ Q_G^{GJ}\ P_J^{GJ}\ Q_J^{GJ}\ Q_J^{JS}\ P_S^{JS}\ P_B^{C3}\ P_D^{CD}\ P_B^{C2}\ P_U^{C3}\ P_K^{KI}\ P_H^{GH}\ P_B^{C1}\ P_U^{C4}\ P_R^{RJ}]^T \end{aligned} \tag{4}$$

Through integrating the two state vectors together, the state vector of the full car with a HIS is obtained

$$X = \left[X_M^T\ X_H^T\right]^{\mathrm{T}} \quad (18{+}34{=}52\ \textit{elements}) \tag{5}$$

Using free body diagram approach and applying Newton's second law, the full car system state space equation is derived

$$T\dot{X} = SX + F\,, \tag{6}$$

$$\begin{bmatrix} I_9 & 0 & 0 \\ 0 & M_9 & 0 \\ 0 & 0 & (T_H)_{34} \end{bmatrix} \begin{bmatrix} \dot{Z} \\ \ddot{Z} \\ \dot{X}_H \end{bmatrix} = \begin{bmatrix} 0 & I_9 & 0 \\ -K & -C & 0 \\ 0 & 0 & S_H \end{bmatrix}_{52X52} \begin{bmatrix} Z \\ \dot{Z} \\ X_H \end{bmatrix}_{52} + \begin{bmatrix} 0 \\ F_M \\ F_H \end{bmatrix}_{52} \tag{7}$$

The external applied forces F_M & F_H include interactive elements between hydraulic or mechanical subsystems. They can be separated into

$$F_M = F_m + S_{H2M} X_H \tag{8}$$

$$F_H = F_h + K_{Z2H} Z + C_{\dot{Z}2H} \dot{Z} \tag{9}$$

That is:

$$\begin{bmatrix} I_9 & 0 & 0 \\ 0 & M_9 & 0 \\ 0 & 0 & (T_H)_{34} \end{bmatrix} \begin{bmatrix} \dot{Z} \\ \ddot{Z} \\ \dot{X}_H \end{bmatrix} = \begin{bmatrix} 0 & I_9 & 0 \\ -K & -C & S_{H2M} \\ K_{Z2H} & C_{\dot{Z}2H} & S_H \end{bmatrix}_{52X52} \begin{bmatrix} Z \\ \dot{Z} \\ X_H \end{bmatrix}_{52} + \begin{bmatrix} 0 \\ F_m \\ F_h \end{bmatrix}_{52} \tag{10}$$

where **M**, **K**, **C** are the mass, stiffness and damping coefficient matrices respectively; S_{H2M}, K_{Z2H}, $C_{\dot{Z}2H}$ are the coefficients matrix coupling the motions of the lumped mechanical system and dynamics of the suspension fluid circuits; S_H is the coefficient matrix determining the dynamics of the fluid circuits.

To obtain the solution of Equation (10), the dynamic state of the multi-body system and that of the fluid circuits can be determined simultaneously using the first 18 equations for the multi-body system and the last 34 equations for the fluid circuits respectively. The following provides a brief description of the modeling and the numerical solution scheme of the fluid circuit dynamics. The assumptions and discussions on the solution scheme can be found in [9-11].

4. FIELD TESTS OF A SUV FITTED WITH A HIS

The experiments that are conducted for handling analysis of HIS system includes roll, pitch and bounce modes tests. In roll mode, slalom tests (sine wave), U turn and 360 degree turn tests are performed at different vehicle speed. The performances of HIS systems with different pre-charged pressures are also tested and compared. Due to the limit of the pages, in this paper only the results of a HIS pre-charged with 40bar in slalom test at 30km/hour vehicle speed is presented. In pylon course slalom test, a 2004 Ford Territory, shown in Figure 3, is driven through a series of pylons which are placed 10m apart. The anti-roll bar has been taken off from the experiment vehicle and replaced with a passive roll-resistant HIS, shown in Figure 5. As a comparison, an original Territory, shown in Figure 4, with anti-roll bars is tested under the same experiment condition.

Figure 3 Pylon course slalom test-HIS car

Figure 4 Pylon course slalom test-standard car

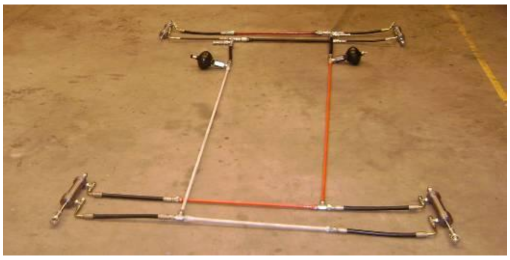

Figure 5 the assembled HIS system

Figure 6 mounting of the accumulator

Four accelerometers are mounted on vehicle chassis to take the measurement in vertical (left and right side of vehicle chassis), longitudinal and lateral directions. Two displacement transducers are mounted along the rear shock absorbers to record suspension travel, as well as two pressure transducers are installed into two hydraulic circuits of HIS respectively to measure the hydraulic pressure change. A LabJack data acquisition module and Labview are used for data acquisition.

5. RESULT COMPARISON AND DISCUSSIONS

In order to excite vehicle roll motion, the vehicle lateral acceleration generated during slalom tests should be adequately large[22; 23]. For accuracy and safety, ideally testing vehicles should be self-driven in a constant high speed, maneuvered by an automatic steering mechanism to conduct the pre-designed maneuver pattern, which is however not available in this case. From a rigid vehicle model we know during cornering vehicle lateral acceleration is mainly determined by steering angle and vehicle speed, apart from ground inputs and tire slipping. To generate the targeted large lateral acceleration and also ensure the safety of testing person, a lower speed but larger steering angle is chosen as experimental strategy for risk management purpose. Overall, the vehicle lateral acceleration in pylon course slalom test goes up to 0.8g at 30km/hour, which is sufficient according to the literature that most vehicles tested for handling evaluations experience a lateral acceleration up to 0.8g. [22; 23]

In order to be comparable, simulations and experiment should run under the same inputs, e.g., steering input. Because of the nature of human driver, it is impossible to exactly follow the pre-designed driving pattern. Hence, the steering angle that measured from experiment is used as steering input to simulation to ensure the simulation run under the same input with experiments. The steering input is shown in Figure 7.

Figure 8-9 present the slalom test results of the experimental vehicle fitted with the HIS, including lateral acceleration and HIS pressure response. Due to the limit of pages, only 40bar HIS in 30km/hour testing data is provided with comparison with simulations. In Figure 8, using the steering angle in Figure 7 as input to vehicle and HIS models, the vehicle lateral acceleration from the simulation matches the acceleration data collected from experiment. It means the steering input that is estimated from tests is of good accuracy to be used as simulation input.

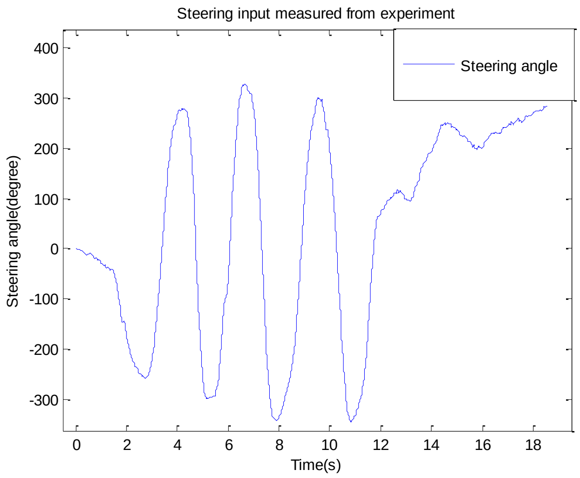

Figure 7 Steering angle input

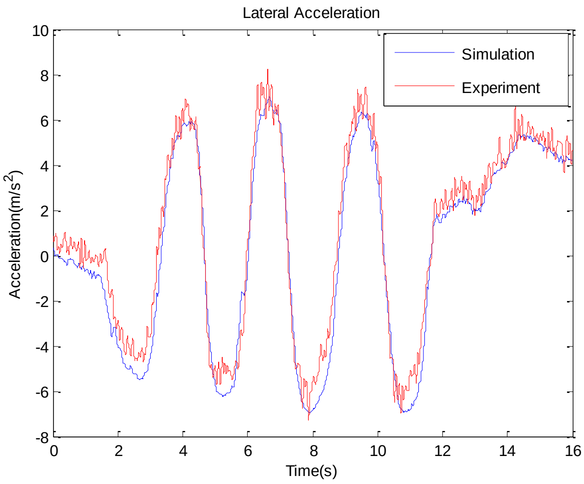

Figure 8 Vehicle lateral acceleration

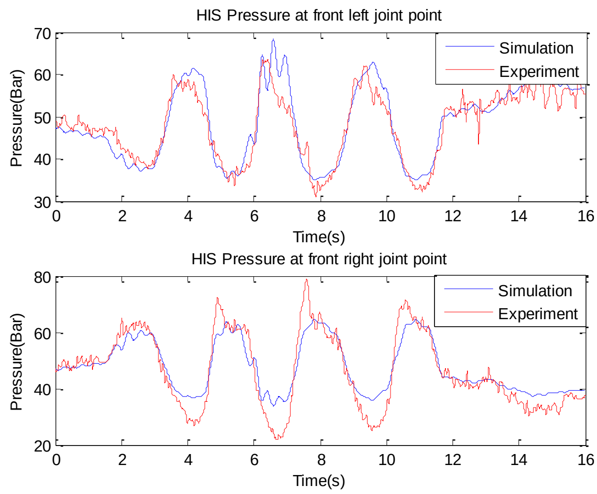

Figure 9 HIS pressure response

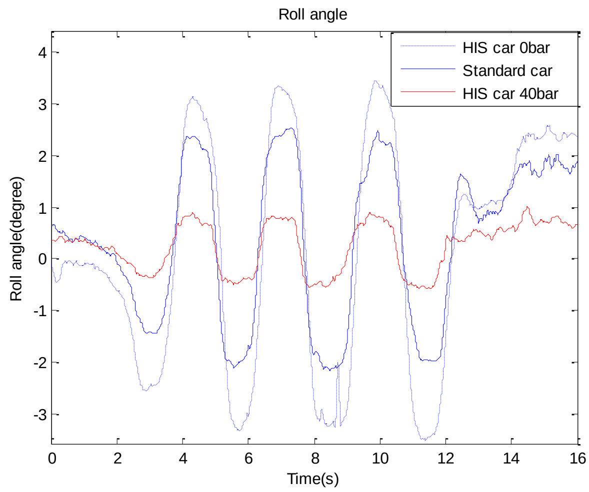

Figure 10 Vehicle roll angle from testing

Apart from acceleration sensors, two pressure sensors are installed into the front left/right joint points of HIS system, the pressure data collected from the experiment is provided in Figure 9, compared with simulations. The HIS system is pre-charged with 40 bar when no payload is on board. However, the system pressure rises to 47bar after loading two testing personal and equipments. This change is considered in simulation. From Figure 9, we can see from the experimental data the right side HIS pressure response is slightly severer than the left side HIS. One possible reason is due to a slightly tilted road surface of 3~5 degree.

Figure 10 compares the performance of hydraulic anti-roll system with anti-roll bars. The vehicle body roll angle is estimated from suspension travels, so this roll angle is smaller than the real vehicle roll angle since the tire deflection is not included. The dashed line is the experimental car with a HIS system pre-charged with 0bar, which means HIS is de-functioned and the car has no active anti-roll systems. Thus the largest vehicle roll motion is expected and witnessed from the graph. This data is used as benchmark to evaluate other anti-roll systems. The blue solid line refers to the standard car with anti-roll bars and it proves the effectiveness of anti-roll bars in vehicle roll control. The third red line refers to the experimental car fitted with the 40bar pre-charged HIS system, and it shows an obvious advantage of HIS over anti-roll bars in minimizing the vehicle roll angle.

6. CONCLUSION

This paper presents the transient handling analyses of an SUV fitted with the hydraulic interconnected suspension with simulation and field tests. The 52 DOF modeling of the car and hydraulic system is briefly provided and the transient simulation results are presented in slalom test. The experimental vehicles are driven through a series of pylons at a constant speed of 30km/hour, and the pre-charged pressure for HIS is 40bar. The measured lateral acceleration and HIS pressure are compared with simulations. The results show a good match and integrated mathematical modeling of car and hydraulic system has finally validated by field test results.

Furthermore, through comparison of HIS and anti-roll bars, the advantage of HIS in vehicle body roll cancellation has been highlighted by the experimental result.

References

[1] Smith, M. & Walker, G. 2005, 'Interconnected vehicle suspension', *Proceedings of the Institution of Mechanical Engineers, Part D: Journal of Automobile Engineering*, vol. 219, no. 3, pp. 295-307.
[2] Cao, D., Rakheja, S. & Su, C.-Y. 2010, 'Roll- and pitch-plane coupled hydro-pneumatic suspension -- Part 1: Feasibility analysis and suspension properties', *Vehicle System Dynamics: International Journal of Vehicle Mechanics and Mobility*, vol. 48, no. 3, pp. 361 - 86.
[3] Zapletal, E. 2000, 'Balanced Suspension', *SAE paper 2000-01-3572*.
[4] Fontdecaba, J. 2002, 'Integral suspension system for motor vehicles based on passive component', *SAE Technical Paper Series*, vol. 2002-01-3105.
[5] Hawley, J.B. 1927, *Shock Absorber and the Like For Vehicles*, vol. 1,647,518, US
[6] Smith, W. 2009, 'An investigation into the dynamics of vehicles with hydraulically interconnected suspensions', Ph.D thesis, University of Technology, Sydney.
[7] Cao, D. 2011, 'Editors' perspectives: road vehicle suspension design,dynamics, and control', *Vehicle System Dynamics*, vol. 49, no. 1–2, pp. 3–28.
[8] Lovins, A.B. & Cramer, D.R. 2004, 'Hypercars((R)), hydrogen, and the automotive transition', *International Journal of Vehicle Design*, vol. 35, no. 1-2, pp. 50-85.
[9] Smith, W.A., Zhang, N. & Hu, W. 2010, 'Hydraulically interconnected vehicle suspension: handling performance', *Vehicle System Dynamics: International Journal of Vehicle Mechanics and Mobility*.
[10] Smith, W.A., Zhang, N. & Jeyakumaran, J. 2010, 'Hydraulically interconnected vehicle suspension: theoretical and experimental ride analysis', *Vehicle System Dynamics: International Journal of Vehicle Mechanics and Mobility*, vol. 48, no. 1, pp. 41-64.
[11] Zhang, N., Smith, W.A. & Jeyakumaran, J. 2010, 'Hydraulically interconnected vehicle suspension: background and modelling', *Vehicle System Dynamics: International Journal of Vehicle Mechanics and Mobility*, vol. 48, no. 1, pp. 17-40.
[12] Wilde, J.R., Heydinger, G.J., Guenther, D.A., Mallin, T. & Devenish, A.M. 2005, 'Experimental evaluation of fishhook maneuver performance of a kinetic suspension system, ' *SAE paper 2005-01-0392*, .
[13] Cao, D., Rakheja, S. & Su, C.-Y. 2010, 'Roll- and pitch-plane-coupled hydro-pneumatic suspension. Part 2: dynamic response analyses', *Vehicle System Dynamics: International Journal of Vehicle Mechanics and Mobility*, vol. 48, no. 4, pp. 507 - 28.
[14] Cao, D., Rakheja, S. & Su, C.-Y. 2006, 'A Generalized Model of a Class of Interconnected Hydro-Pneumatic Suspensions and Analysis of Pitch Properties', *ASME Conference Proceedings*, vol. 2006, no. 47675, pp. 137-46.
[15] Cao, D., Rakheja, S. & Su, C.Y. 2007, 'Roll plane analysis of a hydro-pneumatic suspension with twin-gas-chamber struts', *International Journal of Heavy Vehicle Systems*, vol. 14, no. 4, pp. 355-75.
[16] Cao, D., Rakheja, S. & Su, C.Y. 2008, 'Dynamic analyses of heavy vehicle with pitch-interconnected suspensions', *International Journal of Heavy Vehicle Systems*, vol. 15, no. 2-4, pp. 272-308.
[17] Mace, N. 2004, 'Analysis and synthesis of passive interconnected vehicle suspensions', PhD thesis thesis, Cambridge University.
[18] Cao, D., Rakheja, S. & Su, C.-Y. 2005, 'Comparison of roll properties of hydraulically and pneumatically interconnected suspensions for heavy vehicles, ' *SAE paper 2005-01-3593*, .
[19] Cao, D., Rakheja, S. & Su, C.Y. 2008, 'Pitch plane analysis of a twin-gas-chamber strut suspension', *Proceedings of the Institution of Mechanical Engineers, Part D: Journal of Automobile Engineering*, vol. 222, no. 8, pp. 1313-35.
[20] Wilde, J.R., Heydinger, G.J. & Guenther, D.A. 2006, 'ADAMS simulation of ride and handling performance of kinetic suspension system,' *SAE paper 2006-01-1972*, .
[21] Zhang, N., Wang, L., Hu, W. & Ding, F. 2010, 'Dynamic Characteristics of a Vehicle Fitted with a Roll-Resistant Hydraulically Interconnected Suspension', paper presented to the *The First IFToMM Asian Conference on Mechanism and Machine Science*, Taipei, Taiwan, October 21 - 25, 2010, .
[22] Savkoor, A.R., Happel, H. & Horkay, F. 1999, 'Vehicle handling and sensitivity in transient maneuvers', in J.P. Pauwelussen (ed.), *Vehicle performance: understanding human monitoring and assessment* Swets&Zeitlinger Publishers, Lisse, The Netherlands, pp. pp. 121-47.
[23] Hegazy, S., Rahnejat, H. & Hussain, K. 2000, 'Multi-Body Dynamics in Full-Vehicle Handling Analysis under Transient Manoeuvre', *Vehicle System Dynamics: International Journal of Vehicle Mechanics and Mobility*, vol. 34, no. 1, pp. 1 - 24.